PCCP

Accepted Manuscript

ROYAL SOCIETY OF CHEMISTRY

www.rsc.org/pccp

Evidence of Anti-parallel Dimer Formation of 4-Cyano-4'-Alkyl Biphenyls in Isotropic Cyclohexane Solution

Shunzo Takabatake[1] *and Toshiyuki Shikata** [1,2]

[1]Department of Symbiotic Science of Environment and Natural Resources,
The United Graduate School of Agriculture, Tokyo University of Agriculture and Technology,
3-5-8 Saiwai-cho, Fuchu, Tokyo 183-8509, Japan

[2]Division of Natural Resources and Eco-materials, Graduate School of Agriculture,
Tokyo University of Agriculture and Technology,
3-5-8 Saiwai-cho, Fuchu, Tokyo 183-8509, Japan

*To whom correspondence should be addressed. E-mail address: shikata@cc.tuat.ac.jp

KEYWORDS. 4-cyano-4'-alkylbiphenyl, liquid crystal, anti-parallel dimer, excimer, ground state dimer, dielectric relaxation, fluorescence

ABSTRACT: The formation of anti-parallel dimers of two liquid crystal forming 4-cyano-4'-alkyl biphenyls (*n*CB, *n* = 5 (pentyl) and *n* = 8 (octyl)) was confirmed in an isotropic cyclohexane solution (*n*CB/cH). In addition to high frequency dielectric relaxation (DR) measurements up to 50 GHz, fluorescence emission (FE) experiments in the wavelength range from 280 to 500 nm were carried out to investigate the molecular dynamics of the *n*CB molecules. The DR spectra for solutions at intermediate to high concentrations were composed of two dynamic modes. A fast mode with a relaxation time of ca. 90 ps was assigned to the free rotations of monomeric *n*CB molecules. The slow mode with a relaxation time of ca. 400 ps was attributed to the dissociation process of the anti-parallel dimers ($(n\mathrm{CB})_2$). The Kirkwood factor (g_K), a measure of orientational correlation between the dipole moments of the cyano groups, was markedly less than unity for the slow mode, which demonstrated the formation of anti-parallel dimers, $(n\mathrm{CB})_2$. The equilibrium constant of anti-parallel dimer formation in an isotropic solution, i.e., for the reaction; $2n\mathrm{CB} \leftrightarrow (n\mathrm{CB})_2$, that was determined via the DR data increased with increasing concentration of *n*CB. In an extremely dilute condition, a sharp fluorescence emission signal attributed to the *n*CB monomer was observed at 325 nm in FE spectrum measurements. However, at the moderate to high concentrations used in the DR measurements where the slow mode was clearly observed, a broad FE signal at 390 nm was observed, which was assigned to excimer emission (including emission from the excited ground state dimers). The relative intensity of the excimer emission to the monomer emission significantly increased with increasing concentration. Moreover, the equilibrium constant for the excimer formation reasonably agreed with that of the anti-parallel dimer formation evaluated by the DR data. Consequently, the results of the FE measurements evidently revealed that excimers of *n*CB and the $(n\mathrm{CB})_2$ dimers formed in isotropic solution are identical chemical species.

INTRODUCTION

Because much of modern technology contains at least one liquid crystalline (LC) component, LC materials are of vast importance to our daily lives. LC materials have been incorporated into the displays of a broad range of everyday tools, including television sets, personal computers, and mobile phones. As a result, information technologies have been established that better allow society to conveniently communicate.[1-5] Despite this importance, LC phase formation occurs in materials that possess particular structural characteristics, and the mechanism for this change is not completely understood.

4-cyano-4'-alkyl biphenyls (*n*CBs), such as 4-cyano-4'-pentyl biphenyl (5CB) and 4-cyano-4'-octyl biphenyl (8CB), are well known LC materials and are widely used in LC displays[6,7]. 5CB is a thermo-tropic LC substance that demonstrates an isotropic to nematic LC phase transition at $T_{I\text{-}N}$ = 35 ºC and a nematic LC phase to solid phase transition (melting point) at T_M = 22.5 ºC.[7] 8CB possesses transition temperatures at $T_{I\text{-}N}$ = 40 ºC, $T_{N\text{-}S}$ = 32.5 ºC and T_M = 22 ºC for the isotropic to nematic LC, the nematic LC to smectic LC and the smectic LC to solid phase transitions, respectively.[7] In the smectic LC phase of 8CB occurring in the temperature range between $T_{N\text{-}S}$ and T_M, formation of anti-parallel dimers has been confirmed using scattering experimental techniques[8-10] and scanning tunneling microscopic (STM) observations on a graphite surface.[11] The formed dimers are arranged in a particular direction (uni-axial director) due to strong dipole-dipole interactions between the dipolar cyano groups. Moreover, Smith et al.[12] reported that the solid phase structure of some longer *n*CBs ($n \geq 8$) deposited on flat graphite surfaces showed two-dimensional molecular arrangements made of anti-parallel dimers. Thus, an anti-parallel dimer $(8CB)_2$ is an essential element forming the smectic LC phase in 8CB.

Because the nematic LC phase has a simpler structure than the smectic LC phase and possesses only a uni-axial director and none of the periodically arranged layers observed in the smectic LC phase, it is possible that anti-parallel dimers are not an essential element of the nematic LC phase for all *n*CBs. Leadbetter et al.[10] claimed that a local bilayer structure made of anti-parallel dimers was present in the nematic LC phase of 5CB using X-ray diffraction techniques.

More than a decade ago, the formation of excimers, i.e., excited dimers including excited ground state dimers, in pure, neat 5CB, 6CB and 8CB was investigated using steady state fluorescence spectroscopy and time resolved fluorescence lifetime measurements over a range of temperatures spanning the isotropic to crystalline states.[13-15] Although the monomer fluorescence intensity was much stronger than the excimer intensity in the crystalline state, excimer fluorescence emission became much stronger than the monomer emission at temperatures higher than $T_{M,}$ regardless of other transition temperatures, i.e., $T_{I\text{-}N}$ and $T_{N\text{-}S}$.[13] Because excimers are excited dimers, they possess characteristic spacing and directionality between the two constituent monomers. Thus, it is possible that excimers formed by *n*CB molecules are identical to the anti-parallel dimers detected previously. If so, a substantial increase in excimer fluorescence emission would reveal the presence of anti-parallel dimers ($(nCB)_2$) not only in the smectic LC phase but also in the nematic LC and isotropic phases. These considerations lead to speculation that anti-parallel dimers $(nCB)_2$ may be the essential basic elements for the formation of nematic LC phases in *n*CB systems.

Molecular dynamic (MD) simulations are useful and reliable tools to investigate intermolecular conformations formed by a test system. Fukunaga et al.[16] carried out MD calculations employing a coarse-grained model and clarified both the static structure and some

dynamic properties of 5CB in a nematic LC phase. They concluded that anti-parallel intermolecular associations are formed locally.

Dielectric relaxation (DR) measurements are a useful method to investigate the magnitude of dipole moments and their orientational dynamics in experimental systems.[17-20] The *n*CB molecules bear cyano (–C≡N) groups with a large intrinsic permanent dipole moment of 4.1 ~ 4.75 D[20,21] fixed at the ends of the molecules parallel to the biphenyl group. Thus, a Kirkwood factor (g_K), defined as the ratio of the square of the apparent dipole moment (μ_{app}^2) to the square of the intrinsic dipole moment (μ_0^2), quantitatively demonstrates the magnitude of the orientational correlation between the dipole moments (and also the molecular axes) in samples.[22] There are three possible outcomes: i) when $g_K > 1$, the dipole moments in the sample tend to be aligned parallel to each other, ii) when $g_K = 1$, the dipole moments have no orientational correlation, and iii) when $g_K < 1$, the dipole moments tend to be aligned anti-parallel to each other. In addition because the dipole moments in the *n*CBs are a result of the dipolar cyano groups that are fixed parallel to the biphenyl groups, the DR modes observed in the *n*CB systems are easily assigned to the molecular motions that are relevant to changes in molecular orientation.

In our previous work,[20] the formation of 5CB and 8CB anti-parallel dimers in isotropic benzene solution (*n*CB/Bz) was investigated using dielectric techniques. Fast and slow relaxation modes were observed at ca. 120 and 400 ps, and the strength of a slow mode remarkably increased with increasing *n*CB concentration. Additionally, the Kirkwood factors observed in the isotropic solution were less than unity and substantially decreased with increasing concentration. Thus, we concluded that anti-parallel dimers exist, even in isotropic solution, for both 5CB and 8CB in the work. The fast relaxation mode was assigned to rotation

of the monomeric *n*CB molecules, and the slow mode was assigned to dissociation of the anti-parallel dimers $(nCB)_2$.[20] However, more evident, quantitative additional experimental results other than the dielectric techniques should be necessary to establish the presence of the anti-parallel dimers in isotropic *n*CB solution even at dilute conditions other than the dielectric techniques.

More than a decade ago, Shabatina[23] used infrared (IR) absorption spectra in a wavenumber (*WN*) range from 2200 to 2250 cm^{-1} to monitor the C≡N stretching vibration mode and found that the peak wavenumber was slightly altered upon formation of anti-parallel dimers. Thus, IR measurements in this *WN* range can be used to evaluate the mole fractions of *n*CB molecules forming the anti-parallel $(nCB)_2$ dimers. In our previous work,[20] the formation of anti-parallel dimers of 5CB and 8CB in the isotropic *n*CB/Bz system was also confirmed using the IR techniques proposed by Shabatina[23]. Reasonable agreement between equilibrium constants for anti-parallel dimer formation evaluated using IR and DR data strongly suggest that anti-parallel dimers are present, thereby validating our analysis.[20]

In this study, in addition to DR relaxation measurements over a frequency range up to 50 GHz, FE experiments in the wavelength range from 290 to 500 nm were employed to confirm evidently the formation of 5CB and 8CB anti-parallel dimers in isotropic cyclohexane (cH) solutions. Bz was not used as a solvent because of its relatively strong absorption between 230 and 270 nm and fluorescence emission from 270 to 320 nm[24]. On the other hand, cH does not fluoresce and can dissolve *n*CB molecules to the relatively high concentrations needed to clearly recognize LC phases[21]. Based on the obtained DR and FE data, the dynamics of the *n*CB molecules and the chemical equilibrium between monomeric *n*CB molecules and anti-parallel

(nCB)$_2$ dimers in the isotropic nCB/cH system are discussed in detail as a function of nCB concentration.

2. EXPERIMENTAL

2.1 Materials: 5CB (> 97 %) and 8CB (> 97 %) were purchased from Wako Pure Chemical Industries Ltd. (Osaka) and were used without any further purification. Highly purified cyclohexane, cH, (> 98 %) was purchased from Kanto Chemical Co., Inc. (Tokyo) and was used without purification. 5CB and 8CB were dissolved into cH at several concentrations (c) ranging from 1.01×10^{-6} to 1.30 M and 1.10×10^{-6} to 1.24 M (3.26×10^{-5} to 37.6 wt% and 4.10×10^{-5} to 41.6 wt%) for 5CB and 8CB, respectively. In the dielectric experiments, only solutions from to 0.12 to 1.30 M (or 1.24 M) were used.

2.2 Methods: Dielectric relaxation, DR, measurements were carried out at 25 ºC in a frequency (v) range from 1 MHz to 50 GHz using two measuring systems. In the low frequency range from 1 MHz to 3GHz, an RF LCR METER 4287A (Agilent Technologies, Santa Clara) equipped with a home-made electrode cell with a vacant electric capacitance of C_0 = 660 fF was used. In this measuring system, real and imaginary components (ε' and ε") of the electric permittivity were calculated using the relationships $\varepsilon' = CC_0^{-1}$ and $\varepsilon'' = (G - G_{dc})(\omega C_0)^{-1}$, where C, G, G_{dc}, and ω are the electric capacitance of the sample, the electric conductance of the sample, the direct current conductance of the sample due to the presence of ionic impurity, and the angular frequency given by $\omega = 2\pi v$, respectively. In the high frequency range from 50 MHz to 50 GHz, a dielectric probe kit 8507E consisting of a network analyzer N5230C, ECal module N4693A, and performance probe 05 (Agilent Technologies) was used for the dielectric relaxation

measurements. A three-point calibration procedure using hexane, 3-pentanone, and water as standard materials was carefully performed prior to sample measurements. In this system, ε' and ε'' were automatically calculated using pre-installed software in the dielectric probe system. The calibration procedure is described in detail elsewhere[18,19]. Temperature of the sample solutions was kept at 25 ºC using thermostating equipment controlled by Peltier devices in both the dielectric measuring systems.

Steady state fluorescence spectra for the *n*CB/cH system were recorded at a room temperature (ca. 25 ºC) using a spectrofluorimeter FP-777 (JASCO, Tokyo). Because absorption and fluorescence emission was so strong in the moderate to concentrated regime, most of the excitation light was absorbed in the front of the quartz cell, and fluorescence emission also occurred there. Thus, a regular rectangular (1 cm × 1 cm) quartz cell could not be used. Instead, we used a screw capped quartz cell with an optical length of 1 mm, allowing the sample to be sealed to avoid evaporation of the solvent cH. The quartz cells were fixed at a position at a 45 º angle relative to the incident excitation light so that the excitation light reflected away from the monochrometer used to analyze the fluorescence emission to reduce errors introduced by the strong reflection of the excitation light.

3. RESULTS AND DISCUSSION

3.1 Dielectric Behavior: Figures 1 (a), (b), (c) and (d) show the dielectric spectra for 5CB/cH at $c = 2.0 \times 10^{-1}$ M (6.4 wt%) and 1.30 M (37.6 wt%), and 8CB/cH at $c = 2.4 \times 10^{-1}$ M (8.7 wt%) and 1.24 M (41.6 wt%), respectively, as typical experimental results. Two sets of Debye-type

relaxation functions given by eq 1 with four parameters (relaxation time (τ_j) and strength (ε_j), j = 1 and 2) were necessary to describe the obtained dielectric spectra.

$$\varepsilon' = \sum_{j=1}^{2} \frac{\varepsilon_j}{1+\tau_j{}^2\omega^2} + \varepsilon_\infty, \quad \varepsilon'' = \sum_{j=1}^{2} \frac{\varepsilon_j \tau_j \omega}{1+\tau_j{}^2\omega^2} \tag{1}$$

Solid lines in the figures represent the summation of the constituent Debye-type relaxations, and the broken and dotted lines represent the two component relaxation modes for j = 1 and 2, respectively.

The dependencies of ε_j and τ_j (j = 1 and 2) on c for both the 5CB/cH and 8CB/cH system are shown in Figures 2(a) and (b), and Figures 3(a) and (b). Because the fast relaxation mode j = 1 was found to be independent of the concentration for both 5CB and 8CB, this mode was attributed to the rotational relaxation mode of the monomeric *n*CB molecules.[20] Similar experimental results were obtained in *n*CB benzene solution in our previous study[20]. Although the macroscopic viscosity of benzene (ca. 0.6 mPa·s at 25 ºC) was slightly lower than that of cyclohexane (ca. 0.9 mPa·s at 25 ºC), the τ_1 value for benzene solution (ca. 1.5×10^{-10} s) is slightly longer than that for cyclohexane solution (ca. 0.9×10^{-10} s). Then, we speculate that microscopic viscosity felt by monomeric *n*CB molecules in solution is not controlled by the macroscopic viscosity of a used solvent, but other factors at the molecular (or nano) level such as an affinity between *n*CB and solvent molecules, and solvation effects. On the other hand, the slow mode j = 2 was observed most clearly at moderate to high concentrations and abruptly increased with increasing concentration. Neither the fast nor the slow modes observed in the 5CB and 8CB data could be assigned to rotation about the long molecular axis of the *n*CB

molecules; instead, these modes were assigned to monomer rotation and anti-parallel dimers dissociation $(n\mathrm{CB})_2$, as discussed in the previous study[20].

The Kirkwood factor, g_K, is defined as a ratio of the square of an apparent dipole moment, μ_{app}^2, to the square of the intrinsic dipole moment, μ_0^2, of a tested substance; $g_K = \mu_{app}^2 \mu_0^{-2}$. This parameter is a quantitative measure of the orientational correlation between two dipoles using the molecular axes for the *n*CB molecules described in the introduction. According to Kirkwood and Fröhlich, the square of apparent dipoles, μ_{app}^2, is given by

$$\mu_{app}^2 = \frac{9(\varepsilon_0 - \varepsilon_\infty)(2\varepsilon_0 + \varepsilon_\infty)\varepsilon_v k_B T}{\varepsilon_0(\varepsilon_\infty + 2)^2 c N_A} \quad (2)$$

where ε_0, ε_v, $k_B T$, and N_A represent the electric permittivity at $\omega = 0$ ($\varepsilon_0 = \varepsilon_1 + \varepsilon_2 + \varepsilon_\infty$ for Figures 1(a) and (b)), the electric permittivity of a vacuum, the product of the Boltzmann constant and the absolute temperature, and Avogadro's number, respectively. The value of the intrinsic dipole moment has been reported to be $|\mu_0| = 4.75$ D for 5CB[20,21,25]. The evaluated g_K values noted in Figures 1 (a) and (b) assuming $|\mu_0| = 4.75$ D were close to unity, suggesting weak orientational correlation between dipoles. Consequently, independent of the alkyl chains, the *n*CB molecules demonstrated a dielectric process related to the rotational mode around the shorter molecular axes governed by free rotations, which resulted in $g_K = 1$ for the extremely dilute condition.

The concentration dependence of the g_K values for both the 5CB/cH and 8CB/cH systems assuming $|\mu_0| = 4.75$ D are shown in Figure 4. The g_K value decreased with increasing c from unity at $c = 0$ down to ca. 0.7 at $c = 1.30$ and 1.24 M for 5CB and 8CB, respectively. The c dependence of g_K were also observed for the 5CB/Bz and 8CB/Bz systems[20]. Ghanadzadeh et

al.[21] also observed g_K values of less than 0.7 in 6CB/cH and 7CB/cH systems using static dielectric constant measurements, and they concluded that anti-parallel dimers formed in these systems. The obtained g_K values are substantially less than unity and serve as strong evidence for the formation of anti-parallel dimers in both the 5CB/cH and 8CB/cH systems, especially at moderate to high concentrations. Urban et al.[25] also reported a g_K value less than unity for pure 5CB in an isotropic state, and they discussed the presence of anti-parallel dimers, $(5CB)_2$. Kundu et al.[26] also considered the contribution of anti-parallel $(5CB)_2$ dimers to the DR behavior. Similar dielectric behavior to that shown in Figure 4, i.e., g_K values less than unity, has also been observed in tetrachloromethane (CCl_4) solutions of dimethylsulfoxide (DMSO), which has a relatively large dipole moment of ca. 4.0 D and a strong tendency to form anti-parallel dimers.[27]

According to the previous study,[20] we propose a simple model to describe the c dependence of g_K values based on a simple chemical reaction between monomeric nCB and anti-parallel dimers, $(n\mathrm{CB})_2$, governed by an equilibrium constant (K_d) as schematically depicted in Figure 5.[20,27-29] The equilibrium constant can be calculated using the concentration of monomeric nCB ($[M]$) and anti-parallel dimeric $(n\mathrm{CB})_2$ ($[D] = (c - [M])/2$)

$$K_d = \frac{[D]}{[M]^2} = \frac{c - [M]}{2[M]^2} \qquad (3)$$

The fast dielectric relaxation mode $j = 1$ has been assigned to rotations of monomeric nCB molecules because this motion is the fastest dielectrically active mode.[20] The values of τ_1 seem to range from 70 to 100 ps independent of the concentrations and species of nCB, as observed in Figures 2(b) and 3(b). On the other hand, the slow mode $j = 2$ was assigned to dissociation of the anti-parallel dimers, $(n\mathrm{CB})_2$, governed by the lifetime of the dimers (τ_{life}).[20] Because (perfectly)

anti-parallel dimers possess no dipole moments, rotations of the anti-parallel dimers are dielectrically inert, as schematically described in Figure 5. After the dissociation process, the two monomeric *n*CB molecules that are generated are capable of the quick rotation having a dielectric relaxation with a characteristic time of τ_2 ($\sim\tau_{life}$). According to this model[20], the lifetime, τ_2, of anti-parallel dimers, $(8CB)_2$, in cH does not look so different from that of $(5CB)_2$.

Here, we consider the relationship $\varepsilon_1 = \alpha_M[M]$, where α_M is a proportionality constant obtained by assuming $\boldsymbol{\mu}_{app}^2 = \boldsymbol{\mu}_0^2$, $g_K = 1$ for the monomeric *n*CB and $[M] = c$, i.e., $[D] = 0$, in eq 2.[20] By use of α_M, eq 3 is rewritten as

$$K_d = \frac{\alpha_M^2\left(c - \varepsilon_1/\alpha_M\right)}{2\varepsilon_1^2} \qquad (3')$$

Eq 3' permits the calculation of K_d at each examined concentration, c, from the dielectric relaxation data. The obtained K_d values are plotted as a function of the concentration for the 5CB/cH and 8CB/cH systems in Figure 6(a) and (b), respectively. K_d increased with increasing c irrespective of the *n*CB species. This observation clearly suggests that anti-parallel dimer formation is remarkably enhanced by increasing c, even in an isotropic cH solution, and this increase is especially pronounced at low c. Large amounts of the *n*CB molecules form anti-parallel dimers at a high c, as shown in the molar fraction of $(n\text{CB})_2$ ($f_D = 1 - [M]c^{-1}$) in Figure 6(a) and (b). It seems that most of 5CB and 8CB molecules in the system (greater than 0.9 by molar fraction) form anti-parallel dimers at $c \geq 0.8$ M. The dependence of K_d on c observed in Figure 6 suggest that longer alkyl chains have a stronger tendency to form anti-parallel dimers at low c. The K_d values for 5CB and 8CB in isotropic Bz solution[20] were significantly lower than

those in cH solution over the entire c range examined. These differences in the K_d values seem to be the result of the differences in solubility for the nCB molecules in Bz and cH.

A proportionality constant, α_D, defined as $\varepsilon_2 = \alpha_D[D]$ was also evaluable via an equation $\alpha_D = 2\varepsilon_2(c - [M])^{-1}$. The relationship $\alpha_M > \alpha_D/2$ is responsible for the relationship $g_K < 1$ in both the 5CB/cH and 8CB/cH systems, as was the case for the 5CB/Bz and 8CB/Bz systems[20].

3.2 Fluorescence Behavior: In an extremely dilute condition, the nCB molecules are expected to be isolated and behave as individual molecules in both the 5CB/cH and 8CB/cH systems. The fluorescence emission spectra ($I_{EM}(\lambda)$ vs λ) upon excitation at 274 nm normalized by the emission intensities at 325 nm for the 5CB/cH and 8CB/cH systems over the concentration range from 1.0×10^{-6} (1.1×10^{-6}) to 1.0×10^{-3} (1.1×10^{-3}) M are shown in Figure 7(a). The obtained emission spectra for both systems are essentially independent of concentration and the number of alkyl chains (excluding the small peaks observed at 310 nm), suggesting that the spectra represent emission from nCB monomers. Figure 7(b) shows the excitation spectra ($I_{EX}(\lambda)$ vs λ) for both the 5CB/cH and 8CB/cH systems recorded at the emission wavelength of 325 nm for the same concentrations as in Figure 7(a) normalized by the intensities at the peak wavelength of 274 nm. A weak alkyl chain length dependence is observed, and more notably, the spectra become broader with increasing c. These observations reveal that the fluorescence behavior of the nCB molecules substantially deviates from an expected linear response with changing concentration because of self-absorption approximately 310 nm, even in dilute cH solutions in the absence of excimer.

Fluorescence emission spectra for the 5CB/cH system at moderate to high concentrations (1.0×10^{-2} to 1.30 M) upon excitation at 274 nm normalized to the emission peak intensity are

shown in Figure 8(a). The magnitude of the fluorescence peak found at 325 nm, which corresponds to the monomer emission, clearly decreased. A new peak at 380 ~ 390 nm remarkably increased with increasing *c*. Because the fluorescence emission wavelength of the new peak agreed well with that reported in the literature as excimer emission in the pure, neat 5CB[13-15], this new fluorescence peak was attributed to the excimer emission signal. Excitation spectra normalized by the peak at 270 nm for the monomer and excimer emissions at 325 and 390 nm, respectively, are shown in Figure 8(b). The dependence of the excitation spectra on the emission wavelength is not strong, whereas the dependence on *c* is considerable. The excitation spectra became broader with increasing *c*. These observations suggest that there exist two types of excimers, each possessing different excitation spectra. The first type of excimer is an ordinary excimer generated by a contact between an excited monomer and a ground state monomer, which should possess the same excitation spectra as a monomer and is mainly observed in a system consisting of repulsive monomer molecules. The second type excimer is classified as another excited chemical species that is generated by the excitation of a ground state dimer formed by inter-molecular attractive interactions. These types of interactions are characteristic for a system with dipole-dipole interactions like those in the 5CB/cH system.[13,31] In seminal fluorescence spectroscopic studies on *n*CB carried out on the pure, neat state, classification of excimers was considered but was not taken into account in an explicit manner.[13-15] Because our 5CB/cH system demonstrated excitation spectra rather different from those of the monomers, as observed in Figures 7(b), a large amount of excimers generated in the system are likely excited ground state dimers. Essentially, the same concentration dependence of fluorescence emission and excitation spectra were observed also in the 8CB/cH system at moderate to high concentrations, as observed in Figures 9(a) and (b).

Here, we assume that the *n*CB molecules possess only two states: monomers and excimers (including ground state dimers), in both the 5CB/cH and 8CB/cH systems. In this scenario, the fluorescence emission spectra should remarkably alter depending on the distribution of monomers and excimers because both monomers and excimers have the same excitation peak wavelength of 275 nm. Moreover, emission spectra normalized by the total amount of effectively excited species in the examined system should have an isosbestic point between the monomer and excimer emission wavelength that is independent of the distribution of monomers and excimers. However, the total amount of effectively excited species was not known precisely in this study because of the very large c range that exceeded the region of linear dependence on c due to strong absorption at the front face of the sample and self-absorption by the *n*CB molecules. Fortunately the fluorescence emission spectra at $c = 2.0 \times 10^{-1}$ M demonstrated a clear minima at close to 350 nm as observed in Figure 8(a). Thus, 350 nm was used as the isosbestic point.

If the isosbestic point is known, a standard monomer and dimer, ($I_{EM,M}^{Std}(\lambda)$ and $I_{EM,D}^{Std}(\lambda)$), emission spectra for a given solution can be determined by multiplying the normalized monomer and excimer emission spectra, $I_{EM,M}(\lambda)$ and $I_{EM,E}(\lambda)$, by a correction factor. The normalized emission spectra, $I_{EM}(\lambda)$, of a sample solution can then be described as $I_{EM}(\lambda) = f_M I_{EM,M}^{Std}(\lambda) + f_E I_{EM,E}^{Std}(\lambda)$ where $f_M + f_E = 1$. If the isosbestic point's wavelength, λ_{iso}, is not correctly selected, the relationship $f_M + f_E = 1$ will not be satisfied. Figures 10 shows the values of $f_M + f_E$ calculated for several trial isosbestic point wavelengths, 340, 350, 360 and 370 nm for the 5CB/cH system at some concentrations. The relationship $f_M + f_E = 1$ was best satisfied at 350 nm, revealing that the isosbestic point is near 350 nm in the 5CB/cH system.

Figure 11 shows the fluorescence emission spectra for the 5CB/cH system in the moderate to high concentration regime, which were re-normalized by the emission intensities at

λ_{iso}(=350 nm): $I_{EM}^{350}(\lambda)$. It seems that the monomers dominate the system at $c < 1.1\times10^{-2}$ M, whereas excimers dominate at $c > 8.3\times10^{-1}$ M. Because the shape of the emission spectra approximately 330 nm was reductively influenced by self-absorption phenomenon due to the overlapping of the emission and excitation spectra (cf. Figures 8(a) and (b)), deconvolution of the fluorescence emission spectra near this wavelength into their constituent monomer and excimer components is inaccurate. However, at wavelengths longer than 340 nm, this analysis was reasonably performed by a curve fitting procedure using the emission spectra at $c = 1.1\times10^{-2}$ and 1.3 M as the standard emission spectra for the monomer, $I_{EM,M}^{Std}(\lambda)$, and excimer, $I_{EM,E}^{Std}(\lambda)$, respectively. Then, a ratio of the fraction of excited monomers to that of excited excimers, $f_M f_D^{-1}$, which is identical to the value of $[M](2[D])^{-1}$, was approximately determined. Then, the determined $[M](2[D])^{-1}$ value at each c permitted evaluation of the equilibrium constant (K_e) for the chemical reaction between monomers and excimers via eq 3 (cf. Figure 5). The obtained K_e value for the 5CB/cH is shown also in Figure 7 as a function of c. Agreement between K_d and K_e strongly suggests that the anti-parallel dimer and the excimers (including the excited ground state dimers) are identical chemical species.

In the 8CB/cH system, the influence of the concentration on the emission spectra in the moderate to high concentration regime was much stronger than that of the 5CB/cH system. Thus, the emission intensities around λ_{ex} = 350 nm were strongly reduced due to self-absorption (cf. Figure 9(a)) in the concentrated regime such that K_e evaluation was not performed. However, we believe that the same excimer formation process governed by the chemical equilibrium shown by Figure 5 (cf. eq 3) holds in the 8CB/cH based on the results from the 5CB/cH system.

4. CONCLUSIONS

Liquid crystal forming 4-cyano-4'-pentylbiphenyl and 4-cyano-4'-octylbiphenyl make anti-parallel dimers, even in isotropic cyclohexane solutions, irrespective of the alkyl chains. The formation of anti-parallel dimers is well described as a chemical equilibrium between monomers and dimers, and the equilibrium moves toward dimer formation with increasing concentration. These anti-parallel dimers could then be necessary for the appearance of the nematic liquid crystalline phase at higher concentrations and also in the pure, neat state.

Two types of molecular dynamic processes were dielectrically observed in the isotropic cyclohexane solution for both species. A fast relaxation mode was assigned to a rotational relaxation mode of monomeric molecules, and a slow relaxation mode was attributed to dissociation of the anti-parallel dimers. The slow mode increased the magnitude of the relaxation in proportion to the anti-parallel dimer formed with increasing concentration.

The formation of the anti-parallel dimer in the isotropic solution was also evaluable using fluorescence techniques because the dimer exhibited a clear excimer emission at a wavelength longer than that of the monomer emission. The concentration dependence of the equilibrium constant of the anti-parallel dimer formation process determined using fluorescence techniques demonstrated fairly good agreement with that determined by the dielectric methods. Evidently, the dimers formed in isotropic solution are identical chemical species to the anti-parallel dimers detected by the dielectric relaxation experiments.

ACKNOWLEDGMENT: TS is indebted to The Nippon Synthetic Chemical Industry Co., Ltd. (Osaka) for their kind financial support for this study. This work was partially supported by JSPS Grant-in-Aid for Scientific Research (B) Number 26288055.

REFERENCES

1) Castellano, J. A. *The Story of Liquid Crystal Displays and the Creation of an Industry*; World Scientific: Singapore, 2005.

2) Kawamoto, H. The history of liquid-crystal displays. *Proc. IEEE* **2002**, *4*, 460-500.

3) Heilmeier, G. H.; Zanoni, L. A.; Barton, L. A. Dynamic scattering: A new electrooptic effect in certain classes of nematic liquid crystals. *Proc. IEEE* **1968**, *56*, 1162–1171.

4) Williams, R. Domains in liquid crystals. *J. Phys. Chem.* **1963**, *39*, 382–388.

5) Gray, G. W.; Kelly, S. M. Liquid crystals for twisted nematic display devices. *J. Mater. Chem.* **1999**, *9*, 2037–2050.

6) Collings, P. J.; Hird, M. *Introduction to Liquid Crystals: Chemistry and Physics*; Taylor & Francis: London, 1997; p.51.

7) Gray, G. W.; Harrison, K. J.; Nash, J. A. New family of nematic liquid crystals for displays. *Elect. Lett.* **1973**, *9*, 130–131.

8) Haase1, W.; Fan, Z. X.; Müller, H. J. Order parameter and packing studies in nematic and smectic A phases by x-ray diffraction. *J. Chem. Phys.* **1988**, *89*, 3317-3322.

9) Gierlotka, S.; Lambooy, P.; de Jeu, W. H. X-Ray Reflectivity of Free-Standing Smectic Films. *Europhys. Lett.* 1990, 12, 341-345.

10) Leadbetter, A. J.; Richardson, R. M.; Colling, C. N. The Structure of a Number of Nematogens. *J. Phys. Colloques* **1975**, *36*, C1-37–C1-43.

11) Foster, J. S.; Frommer, J. E. Imaging of liquid crystals using a tunnelling microscope. *Nature* **1988**, *333*, 542-545.

12) Smith, D.P.E.; Hörber, H.; Gerber, Ch.; Binnig, G. Smectic Liquid Crystal Monolayer on Graphite Observed by Scanning Tunneling Microscopy. *Science* **1989**, *245*, 43-45.

13) Ikeda, T.; Kurihara, S.; Tazyke, S. Excimer Formation Kinetics in Liquid-Crystalline Alkylcyanobiphenyls. *J. Phys. Chem.* **1990**, *94*, 6550-6555.

14) Piryatinskiĭ, Y. P.; Yaroshchuk, O. V. Photoluminescence of Pentyl-Cyanobiphenyl in Liquid-Crystal and Solid-Crystal State. *Opt. Spectrosc.* **2000**, *89*, 860-866.

15) Abe, K.; Usami, A.; Ishida, K.; Fukushima, Y.; Shigenari, T. Dielectric and Fluorescence Study on Phase Transitions in Liquid Crystal 5CB and 8CB. *J. Korean Phys. Soc.* **2005**, *46*, 220-223.

16) Fukunaga, H.; Takimoto, J.; Doi, M. Molecular dynamic simulation study on the phase behavior of the Gay-Berme model with a terminal dipole and a flexible tail. *J. Chem. Phys.* **2004**, *120*, 7792-7800.

17) Dunmur, D. A.; Luckhurst, G. R.; de la Fuente, M. R.; Diez, S.; Peréz Jubindo, M. A. Dielectric relaxation in liquid crystalline dimers. *J. Chem. Phys.* **2001**, *115*, 8681-8691

18) Ono, Y.; Shikata, T. Hydration and Dynamic Behavior of Poly(N-isopropylacrylamide)s in Aqueous Solution: A sharp Phase Transition at the Lower Critical Solution temperature. *J. Am. Chem. Soc.* **2006**, *128*, 10030-10031.

19) Satokawa Y.; Shikata, T. Hydration Structure and Dynamic Behavior of Poly(vinyl alchol)s in Aqueous Solution. *Macromolecules* **2008**, *414*, 2908-2913.

20) Shikata, T.; Megumi, M. Anti-parallel Dimer Formation of 4-Cyano-4'-Alkyl Biphenyls in Isotropic Benzene Solution. *Nihon Reoroji Gakkaishi* **2014**, *42*, 197-206.

21) Ghanadzadeh, A.; Beevers, M. S. Dielectric investigations and molecular association in non-mesogenic and mesogenic solutions. *J. Mol. Liq.* **2003**, *102*, 365-377.

22) Kirkwood, J. D. The Dielectric Polarization of Polar Liquids. *J. Chem. Phys.* **1937**, *7*, 911-919.

23) Shabatina, T. I.; Vovk, E. V.; Andreev, G. N.; Bogomolov, A. Y.; Sergeev, G. B. IR Spectroscopic Study of Molecular Associations of Mesogenic Cyanophenyls, *J. Struct. Chem.* **1998**, *39*, 318-322.

24) Berlman, I. B. *Handbook of Fluorescence Spectra of Aromatic Molecules*; 2nd Ed. Academic Press: New York and London: 1971; Chap. 4.

25) Urban, S.; Gestblom, B.; Dąbrowski, R. Comparison of the dielectric properties of 4-(2-methylbutyl)-4'-cyanobiphenyl (5*CB) and 4-pentyl-4'-cyanobiphenyl (5CB) in the liquid state. *Phys. Chem. Chem. Phys.* **1999**, *1*, 4843-4846.

26) Kundu, S. K.; Okudaira, S.; Kosuge, M.; Shinyashiki, N.; Yagihara, S. Broadband dielectric spectroscopy of a nematic liquid crystal in benzene. *J. Chem. Phys.* **2008**, *129*, 164509-1-164509-6.

27) Shikata, T.; Sugimoto, N. Reconsideration of the Anomalous Dielectric Behavior of Dimethyl Sulfoxide in the Pure Liquid State. *Phys. Chem. Chem. Phys.* **2011**, *13*, 16542-16547.

28) Shikata, T.; Sugimoto, N.; Sakai, U.; Watanabe, J. Dielectric Behavior of Typical Benzene Monosubstitutes, Bromobenzene and Benzonitrile. *J. Phys. Chem. B* **2012**, *116*, 12605-12613.

29) Shikata, T.; Sakai, Y.; Watanabe J. Nitrobenzene anti-parallel dimer formation in non-polar solvents. AIP Advances **2014**, *4*, 067130-1-13.

30) Reynders, P.; Kuehnle, W.; Klaas, A.; Zachariasse, K. A. Ground-state dimers in excimer-forming bichromophoric molecules. 1. Bis(pyrenylcarboxy)alkanes. *J. Am. Chem. Soc*. **1990**, *112*, 3929-3939.

FIGURE CAPTIONS

Figure 1. Dielectric spectra, ε' and ε'' vs ω, for 5CB/cH at $c = 2.0 \times 10^{-1}$ (a) and 1.30 M (b), and 8CB/cH at $c = 2.4 \times 10^{-1}$ (c) and 1.24 M (d).

Figure 2. Dependence of relaxation strength, ε_1 and ε_2 (a), and times, τ_1 and τ_2 (b), on the concentration, c, for the 5CB/cH system.

Figure 3. Dependence of ε_1 and ε_2 (a) and τ_1 and τ_2 (b) on c for the 8CB/cH system.

Figure 4. Dependence of the Kirkwood factor, g_K, on c for the 5CB/cH and 8CB/cH systems.

Figure 5. Schematic depiction of the chemical reaction between monomeric nCB and anti-parallel dimeric, $(n\text{CB})_2$; $n = 5$ in this depiction.

Figure 6. Dependence of the equilibrium constants: K_d (anti-parallel dimers; circles) and K_e (excimers; triangles), on c for the 5CB/cH (a) and 8CB/cH (b) systems. The c dependence of the anti-parallel dimer mole fractions, f_D (=1-[nCB]c^{-1}; squares), are also plotted. Lines are guides for eyes.

Figure 7. (a): Fluorescence emission spectra ($I_{EM}(\lambda)$ vs λ) normalized by the intensities at 325 nm for the 5CB/cH and 8CB/cH systems at concentrations ranging from 1×10^{-6} to 1.0×10^{-3} M (excitation at 274 nm), and (b): fluorescence excitation spectra ($I_{EX}(\lambda)$ vs λ) normalized by the intensities at 274 nm for the same systems in (a) (emission monitored at 325 nm).

Figure 8. (a): Fluorescence emission spectra, $I_{EM}(\lambda)$ vs λ, normalized by the peak intensities for the 5CB/cH systems at concentrations ranging from 1×10^{-2} to 1.30 M (excitation at 274 nm), and (b): fluorescence excitation spectra, $I_{EX}(\lambda)$ vs λ, normalized by the peak intensities at 274 nm for the same systems in (a) (emission monitored at 325 and 390 nm).

Figure 9. (a): Fluorescence emission spectra, $I_{EM}(\lambda)$ vs λ, normalized by the peak intensities for the 8CB/cH systems concentrations ranging from 1×10^{-2} to 1.24 M (excitation at 274 nm), and (b): fluorescence excitation spectra, $I_{EX}(\lambda)$ vs λ, normalized by the peak

intensities at 274 nm for the same systems in (a) (emission monitored at 325 and 390 nm).

Figure 10. Wavelength dependence of the total fractions of monomers and excimers, $f_M + f_E$, calculated by assuming each λ value as the isosbestic point for the 5CB/cH system at several c values.

Figure 11. Fluorescence emission spectra, $I_{EM}^{350}(\lambda)$ vs λ, re-normalized by intensities at 350 nm for the 5CB/cH system at concentrations ranging from 1.1×10^{-2} to 1.3 M (excitation at 274 nm).

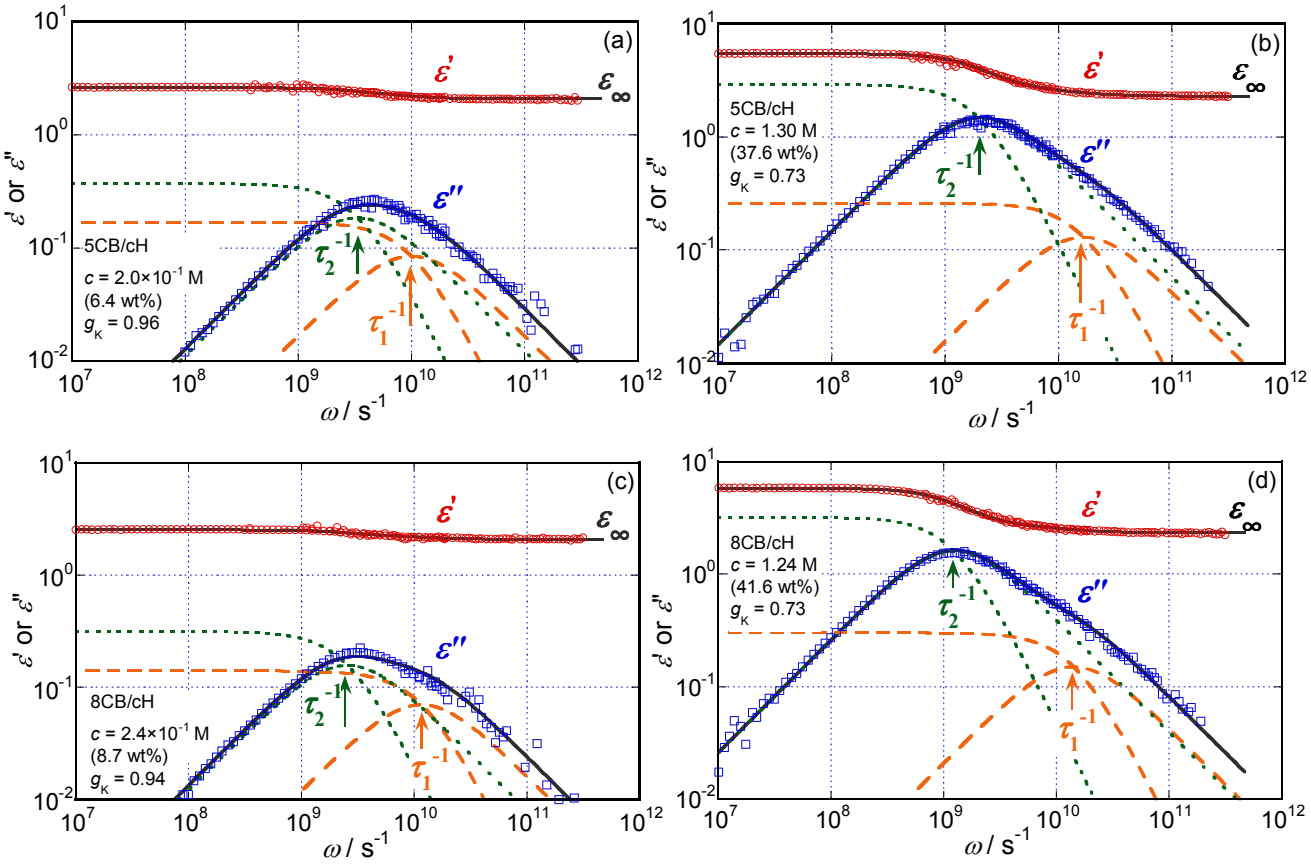

Figure 1

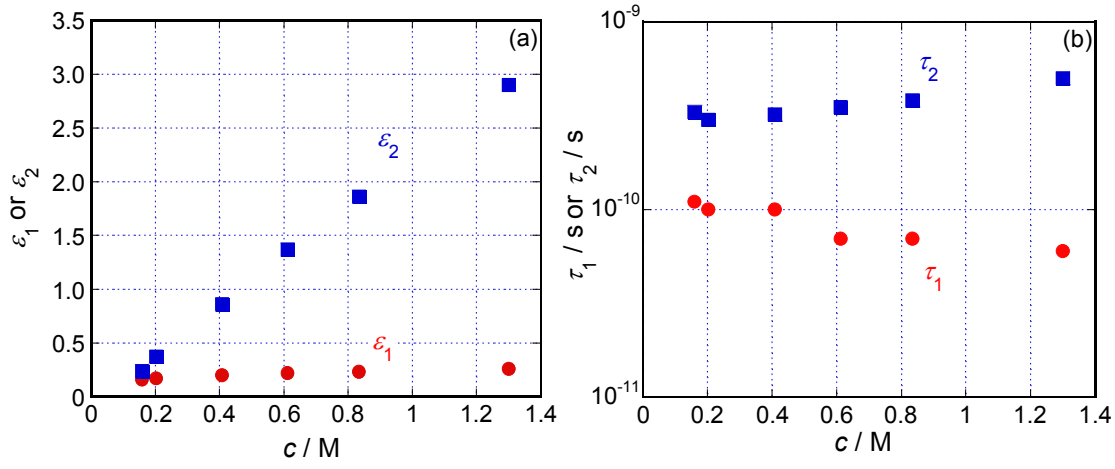

Figure 2

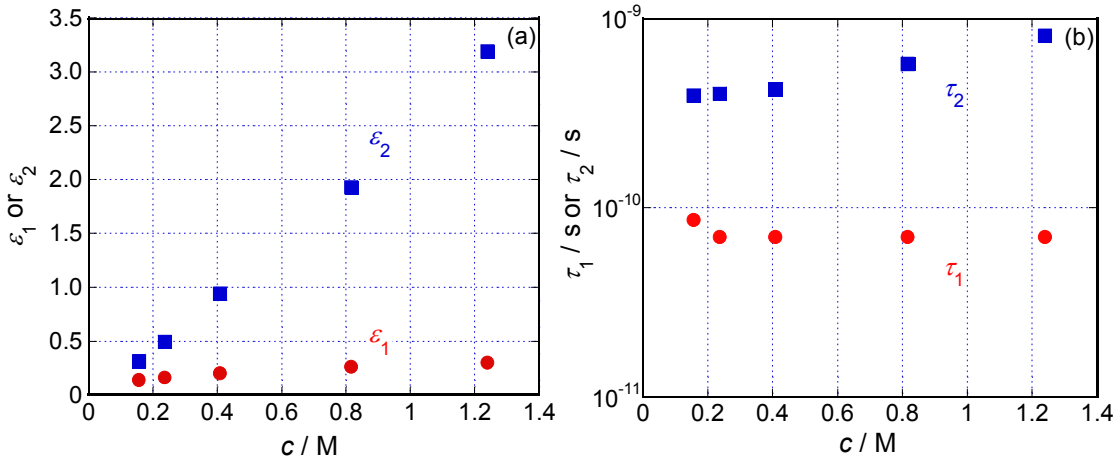

Figure 3

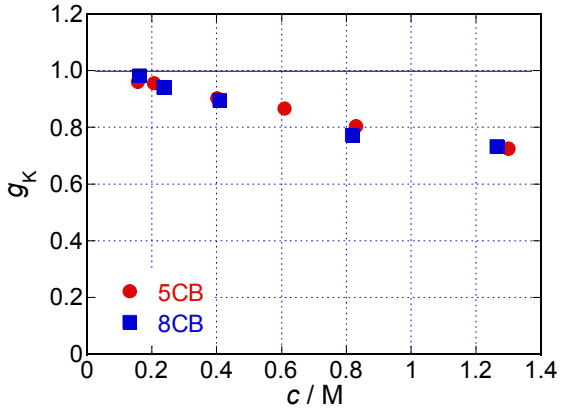

Figure 4

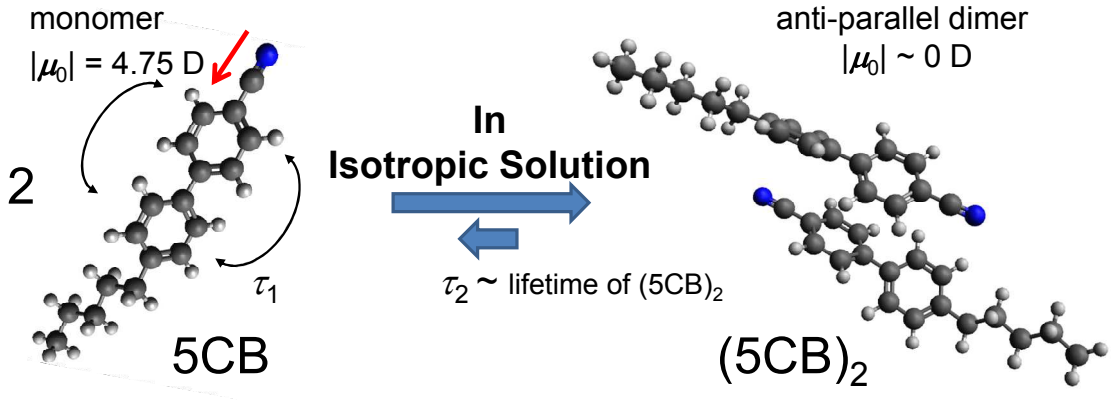

Figure 5

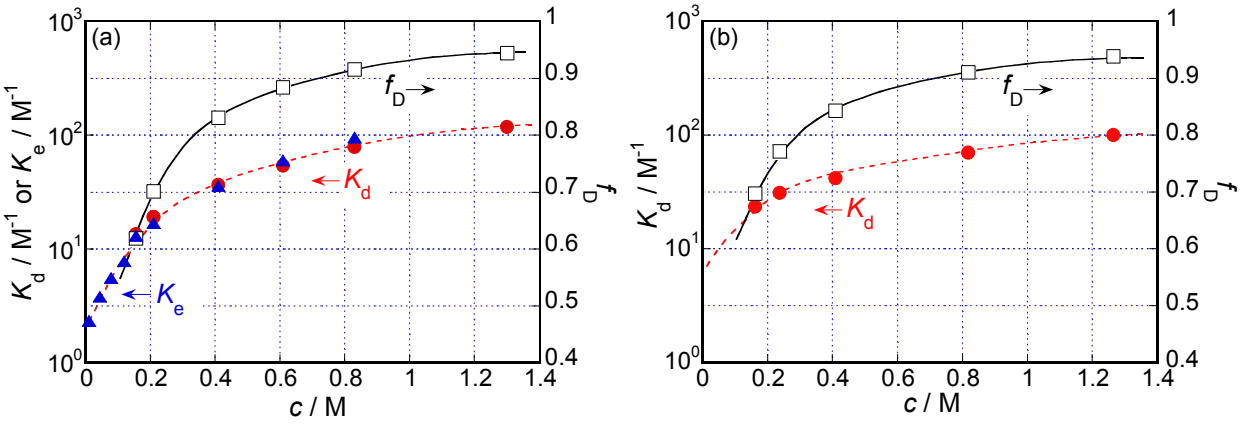

Figure 6

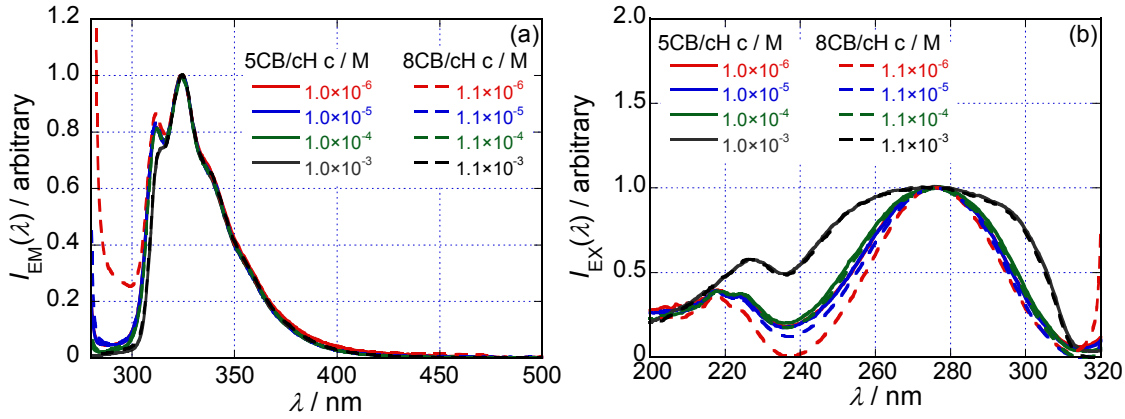

Figure 7

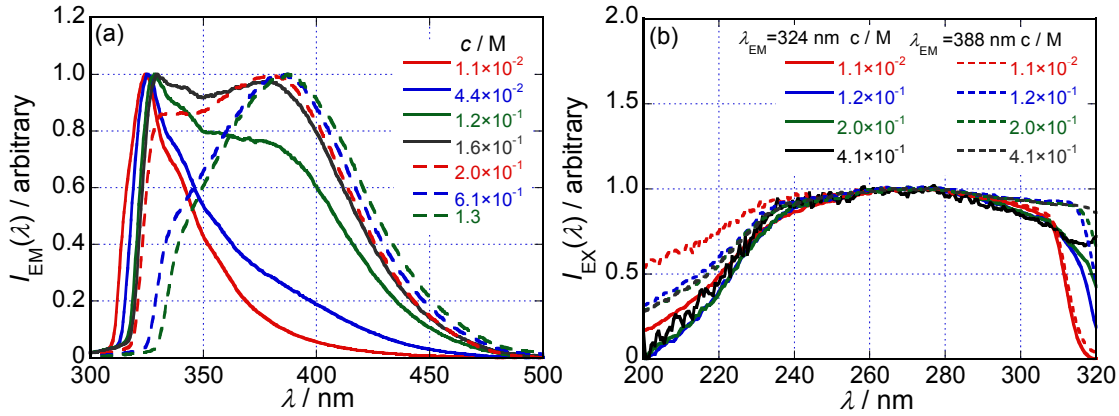

Figure 8

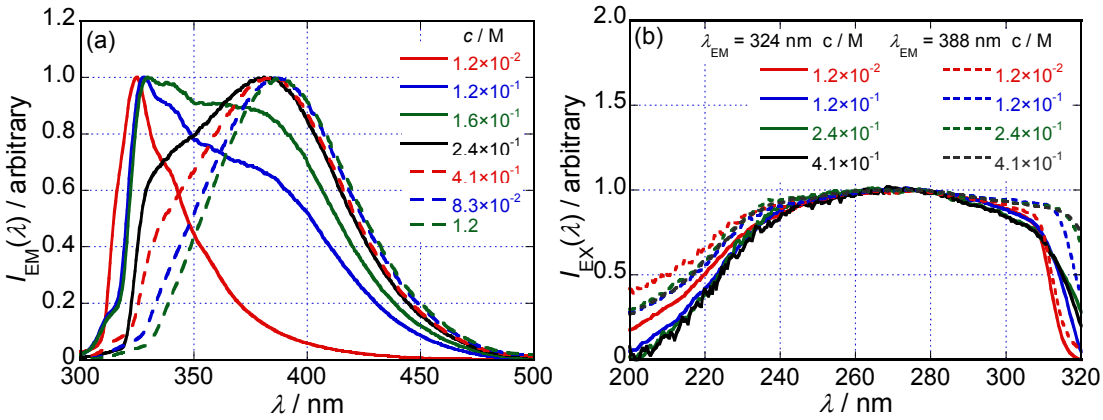

Figure 9

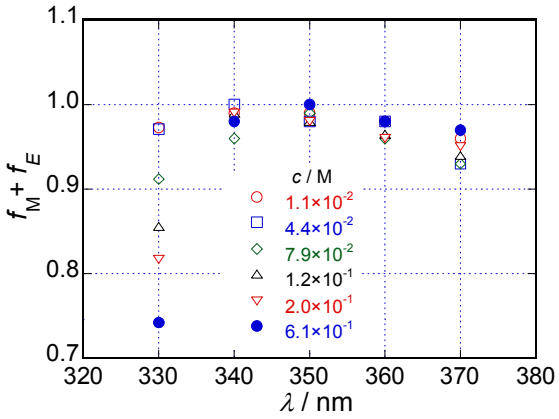

Figure 10

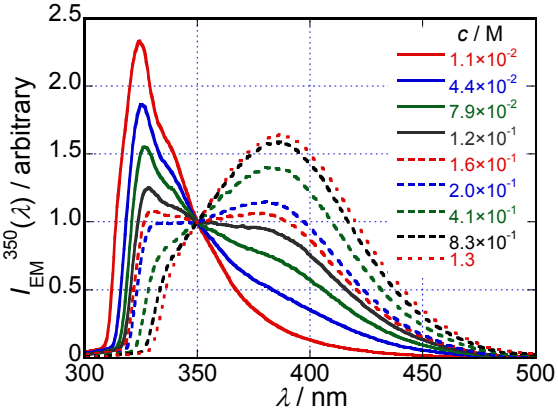

Figure 11